AJNR

Effect of Thin-Section Diffusion-Weighted MR Imaging on Stroke Diagnosis

Hisao Nakamura, Kei Yamada, Osamu Kizu, Hirotoshi Ito, Sachiko Yuen, Takaaki Ito, Kenji Yoshikawa, Kensuke Shiga, Masanori Nakagawa and Tsunehiko Nishimura

AJNR Am J Neuroradiol 2005, 26 (3) 560-565
http://www.ajnr.org/content/26/3/560

Effect of Thin-Section Diffusion-Weighted MR Imaging on Stroke Diagnosis

Hisao Nakamura, Kei Yamada, Osamu Kizu, Hirotoshi Ito, Sachiko Yuen, Takaaki Ito, Kenji Yoshikawa, Kensuke Shiga, Masanori Nakagawa, and Tsunehiko Nishimura

BACKGROUND AND PURPOSE: **Diffusion-weighted (DW) imaging has limited spatial resolution, especially in the *z* direction. We decreased the section thickness of DW imaging to 3 mm to determine if this change improves the depiction of small infarcts and if it affects stroke diagnosis.**

***METHODS*: We studied conventional (5-mm section thickness, 1-mm intersection gap) and thin-section (3-mm section thickness, no intersection gap) DW imaging data in 49 patients with symptoms of acute cerebral ischemia. Two radiologists who were not aware of the clinical findings reviewed all images and diagnosed the stroke subtype according to the Trial of Org 10172 in Acute Stroke Treatment (TOAST) method. Accuracies of stroke diagnosis with an experienced neuroradiologist and with a second-year radiology resident were compared. To quantify lesion conspicuity, contrast-to-noise ratios (CNRs) were measured. The CNR of thin-section DW imaging was then divided by the CNR of conventional DW imaging to yield the relative CNR (rCNR).**

RESULTS: **The experienced neuroradiologist made the correct final diagnoses in 78% of cases with conventional DW imaging, improving to 100% with thin-section DW imaging. The resident made the correct diagnoses in 71% of cases with conventional DW imaging, improving to 94% with thin-section DW imaging. Lesion conspicuity was improved on thin-section DW imaging (rCNR = 1.47 ± 0.63), especially for supratentorial lesions (rCNR = 1.51 ± 0.63).**

CONCLUSION: **Compared with conventional DW imaging, thin-section DW imaging permitted better lesion conspicuity and more precise stroke diagnosis.**

Diffusion-weighted (DW) imaging can demonstrate cerebral infarctions within minutes of their onset and has rapidly become the mainstay in the diagnostic evaluation of patients with stroke (1). Normal random motion of water molecules in the brain results in greater diffusion and loss of signal intensity. Restriction of water movements in areas of infarcted tissue results in less diffusion and increased signal intensity relative to the surrounding normal tissues (2). One of the main roles of neuroimaging studies is to depict these areas of increased signal intensity on DW imaging and to permit estimation of the underlying etiology of stroke (3).

Conventional DW imaging uses 5–8-mm sections with a field of view of 20–40 cm and a matrix of 128–256 (4, 5), which produces in-plane resolution of 1–2 × 1–2 mm. Therefore, the in-plane resolution of DW imaging is higher than the section thickness. When a lesion is smaller than the section thickness and when it occupies only part of a voxel, the contrast relative to background tissue depends on both the signal intensity from the lesion and the proportion of the voxel that it occupies. Small, low-contrast lesions occupying only part of a voxel may go undetected. This phenomenon is known as partial volume averaging or partial volume effect (6, 7). The use of thinner sections may allow small, low-contrast lesions to be detected. Thin-section DW imaging may improve the depiction of smaller infarcts, which may have direct effect on the diagnosis of stroke subtype.

Early subtype diagnosis is of substantial clinical value (8). It aids early prognostication and in identifying patients at increased risk of early neurologic worsening, early recurrent stroke, medical complications, or long-term disability requiring discharge to a long-term care facility (9). Long-term secondary prevention therapies differ substantially for the ischemic stroke subtypes. Early subtype diagnosis allows for

Received December 23, 2003; accepted after revision June 15, 2004.

From the Departments of Radiology (H.N., K. Yamada, O.K., H.I., S.Y., T.I., T.N.) and Neurology (K. Yoshikawa, K.S., M.N.), Kyoto Prefectural University of Medicine, Kajii-cyo, Kawaramachi Hirokoji Noboru, Kamigyo-ku, Kyoto City, Japan.

Address reprint requests to Hisao Nakamura, MD, PhD, Department of Radiology, St. Marianna University of Medicine, Kawasaki City, Kanagawa, Japan 216-8511.

early planning and implementation of appropriate long-term therapy and early hospital discharge. In addition, many clinicians tailor strategies for acute stroke treatment to the stroke subtype.

We hypothesized that the thin-section DW imaging improves the detectabilty of lesions, thereby improving the early subtype diagnosis of brain infarcts. We investigated the utility of the thin-section DW imaging with a 3-mm section thickness by comparing its lesion detectabilty with that of conventional 5-mm section DW imaging. The signal-to-noise ratio of thin-section DW imaging was adjusted to that of conventional DW imaging to enable the observation of the effect of partial volume averaging alone.

Methods

This study was approved by an institutional review board, and written informed consent was obtained from each patient or his or her next of kin. Between October 2001 and January 2003, MR imaging was performed in 250 patients with suspected stroke. Thin-section DW imaging was routinely added to our stroke protocol during this time. After an enrollment period of 15 months, we analyzed the images of all patients who were imaged at the acute stage of infarct. The interval between stroke onset and MR imaging examination ranged from 2 hours to 8 days. The study population consisted of 49 patients (36 men and 13 women; mean age, 68.1 ± 10.6 years; age range, 46–90 years). All infarcts were confirmed to have a decreased apparent diffusion coefficient (ADC) on the ADC maps.

Image Evaluation

All MR images, including DW images, conventional MR images, and MR angiograms were viewed in retrospective fashion. Assessments of conventional and thin-section DW images were done on different days, and the order of the cases was randomized to prevent bias. An experienced neuroradiologist (O.K.) and a second-year radiology resident (T. I.) independently reviewed the images. These physicians knew that the patient had an acute stroke, but they were blinded to the patient's name, clinical presentation, symptoms, and final diagnosis of stroke subtype.

The final clinical diagnosis incorporated information from the MR studies, including the thin-section DW imaging, and also from the patient's subsequent clinical course and results of additional diagnostic tests, including Venereal Disease Research Laboratory (VDRL) slide test, a cholesterol panel, and transthoracic echocardiography. In select patients, findings from transesophageal echocardiography, transcranial Doppler, carotid sonography, cerebral angiogram, CSF testing, and specialized laboratory tests (including hematologic, serologic, and histologic assays) were also included.

Stroke subtype classifications were done in cooperation with neurologists (Y.K., S.K.) according to the categorization of Trial of Org 10172 in Acute Stroke Treatment (TOAST), as follows: 1) large-artery atherosclerosis, 2) cardioembolism, 3) small-artery occlusion, 4) other determined etiology, or 5) undetermined etiology. A detailed algorithm for determining TOAST stroke subtype diagnosis cans be found elsewhere (3).

MR Imaging Protocol

All MR examinations were performed by using a 1.5T clinical imaging system (Gyroscan Intera; Philips Medical Systems, Best, the Netherlands). The routine stroke protocol at our institute requires approximately 14 minutes and consists of the following: conventional DW imaging, T1-weighted imaging (TR/TE, 611/13), T2-weighted imaging (TR/TE, 4754/100), fluid-attenuated inversion recovery imaging (TR/TE/TI, 8000/100/2200), T2*-weighted imaging (TR/TE, 666/23), MR angiography (TR/TE, 30/2.3), and if applicable dynamic susceptibility-contrast perfusion imaging with single-shot spin-echo echo-planar imaging (TR/TE, 1500/90) (10). Conventional DW imaging was performed with a 5-mm section thickness and 1-mm intersection gaps, with a b value of 1000 s/mm^2 and a TR/TE/NEX of 3333/95/2. The entire brain was imaged in 22 axial sections.

Thin-section DW images were obtained with a 3-mm section thickness and 0-mm intersection gaps. The b-value was 800 s/mm^2 with a TR/TE/NEX of 6000/88/6. The entire brain was imaged in 36 axial sections.

Both conventional and thin-section DW imaging were acquired by using three orthogonal gradients in six directions. The recorded data points were 128 × 53 by using the parallel imaging technique, which allowed for image reconstruction by using half encoding steps. Therefore, the true resolution of the images was equivalent to 128 × 106. The data were zero-filled to generate images with spatial resolution of 128 × 128. Total imaging time for conventional DW imaging was 1 minute 28 seconds and that for thin-section DW imaging was 4 minutes 24 seconds. The field of view was 230 × 230 mm. Therefore, the pixel size was 1.8 × 1.8 × 3 mm for thin-section DW imaging and 1.8 × 1.8 × 5 mm for conventional DW imaging.

Image Analysis

Measurements of contrast-to-noise ratio (CNR) were performed to quantify the lesion conspicuity. CNR was calculated as follows: $CNR_{\text{thin-section DW imaging}} = (S_{\text{lesion}} - S_{\text{normal}})/SD_{\text{noise}}$, and $CNR_{\text{conventional DW imaging}} = (S_{\text{lesion}} - S_{\text{normal}})/SD_{\text{noise}}$, where S_{lesion} is the signal intensity of the lesion, S_{normal} is the signal intensity of normal-appearing brain tissue in the contralateral hemisphere, and SD_{noise} is the standard deviation of background noise. The former result was divided by the latter to yield the relative CNR (rCNR).

A neuroradiologist (H.N.) placed the region of interest on each lesion. A second region of interest of the same size was chosen on normal-appearing brain tissue in the same anatomic location on the contralateral, unaffected side of the brain. The size of the region of interest ranged from 26.72 to 153.64 mm^2 (mean, 82.61 mm^2).

To compare the image quality, a signal-to-noise (SNR) measurement was also performed. The SNR was calculated as follows: $SNR_{\text{conventional DW imaging}} = S_{\text{normal}}/SD_{\text{noise}}$, and $SNR_{\text{thin-section DW imaging}} = S_{\text{normal}}/SD_{\text{noise}}$.

Statistical Analysis

Differences between the means for $CNR_{\text{thin-section DW imaging}}$ and $CNR_{\text{conventional DW imaging}}$ were assessed with the paired Student t test. Results were considered significant at $P < .01$. The ability to diagnose stroke subtype differences with the thin-section DW imaging and with conventional DW imaging was analyzed by using the χ^2 test. Results were considered statistically significant at $P < .05$. Interobserver agreement was determined by using kappa statistics.

Results

Increased sensitivity for lesion detection was observed for both the second-year resident and the experienced neuroradiologist. For the resident, sensitivities were 76% and 94%, respectively, for conventional and thin-section DW imaging; sensitivities for the experienced neuroradiologist were 78% and 100%, respectively. Interobserver agreement was good for both the conventional DW imaging (κ = 0.938) and thin-section DW imaging (κ = 0.9111).

TABLE 1: Distribution of stroke subtypes

Stroke Mechanism	No. of Patients (%)
Large-artery atherosclerosis	26 (53)
Cardiogenic embolism	3 (5)
Small-artery occlusion	15 (31)
Other determined etiology	5 (10)

Table 1 summarizes the final consensus diagnoses of stroke subtype according to TOAST classification. The subtype diagnostic accuracy based on image interpretation was as follows: for the second-year radiology resident, 35 (71%) of 49 on conventional DW imaging and 46 (94%) of 49 on thin-section DW imaging, and for the experienced neuroradiologist, 38 (78%) of 49 on conventional DW imaging and 49 (100%) of 49 on thin-section DW imaging. Both readers had significantly higher diagnostic accuracy with thin-section DW imaging than with conventional DW imaging ($P < .05$); this finding indicated that thin-section DW imaging offered higher diagnostic value than conventional DW imaging independent of the reader's experience.

Table 2 summarizes the cases in which the experienced neuroradiologist changed the diagnosis upon seeing thin-section DW imaging data. In three cases (patients 8–10), the thin-section DW imaging depicted an additional lesion in a different vascular territory; this finding altered the diagnosis to a cardiogenic event. In seven cases (patients 1–7), results of conventional DW imaging were negative, but thin-section DW imaging depicted a focus of hyperintensity, which changed the diagnosis from normal to cardioembolic infarction or small-artery occlusion. Figures 1 and 2 illustrate representative cases.

Lesion conspicuity was generally higher with thin-section DW imaging (rCNR = 1.47 ± 0.63) than with conventional DW imaging ($P < .001$), especially for supratentorial lesions (rCNR = 1.51 ± 0.63, $P < .001$) and somewhat for posterior fossa lesions (rCNR = 1.02 ± 0.42) ($P = .3267$). Measured SNRs were comparable for conventional DW imaging (37.3 ± 13.6) and thin-section DW imaging (40.8 ± 14.0).

Discussion

The diagnosis of stroke subtype affects the prognosis, outcome, and choice of management (8, 11). The current approach in stroke care is to implement treatment as rapidly as possible. Outcomes and the likelihood of recurrent stroke remarkably differ among stroke subtypes. For example, cardioembolic stroke is distinct from other groups because its short- and long-term prognoses are generally better. Using thin-section DW imaging, we were able to treat our 11 patients properly (Table 2). With only conventional DW imaging, seven patients would have been regarded as having normal findings and would have not received proper medical treatment. In three other cases, cardioembolic infarction was diagnosis on the basis of thin-section DW imaging results. Cardiac examination was carried out without delay in these cases and lead to prompt confirmation of the diagnosis.

Although the diagnosis of stroke subtype is important, the TOAST study showed that initial diagnosis matched the final diagnosis in only 62% of cases (12). DW imaging may assist in the early diagnosis of stroke subtype because it can render ischemic fields within minutes to hours of ischemia onset (13, 14). To further improve diagnostic accuracy, an even more precise method may be needed. Although DW imaging is a powerful diagnostic tool for investigating stroke etiology, a major drawback is its limited spatial resolution (3). The inherently low spatial resolution of DW imaging in its section plane, compared with that of other MR imaging techniques, has been reported, but the true limitation is its section thickness because its in-plane resolution is far smaller than the section thickness regularly used for MR imaging. Therefore, by decreasing the section thickness, the images more closely approximate isotropic images, improving the detection of small lesions. Our results confirmed this method. SNR is directly proportional to section thickness (15) if all other parameters are the same. By using 3-mm sections instead of 5-mm sections, the SNR of thin-section DW imaging decreased to 3/5, or 60%, in our study. To compensate for this decreased SNR, we tripled the NEX, which increased the SNR by $\sqrt{3}$(71%), or $SNR_{original} \times 0.6 \times \sqrt{3} = 1.04$. Although the b value slightly differed ($b = 800$ s/mm^2 for thin-section DW imaging and $b = 1000$ s/mm^2 for conventional DW imaging), our thin-section DW imaging technique was considered largely comparable with that of conventional DW imaging.

The measured rCNR indicated higher lesion conspicuity for thin-section DW imaging than with conventional DW imaging. However, the standard deviation for this rCNR was relatively large. This can be explained by susceptibility effects from the base of the brain, particularly where air in the sinuses and mastoid bones is near the brain (16). rCNRs were 1.02 ± 0.42 due to the susceptibility effect from the paranasal sinuses, especially with posterior fossa infarcts. Because thin-section DW imaging tended to improve conspicuity of posterior fossa lesions, we believe that the reason for not being able to demonstrate higher CNR for posterior fossa lesions was simply higher background noise and the small number of such lesions.

In this study, the data likely caused underestimation of the usefulness of thin-section DW imaging in stroke subtype diagnosis. Our analysis demonstrated only the effect of thin-section DW imaging on changing the diagnosis of stroke subtype and not its effect in strengthening the likelihood of infarct, owing mainly to higher lesion conspicuity. In addition, we had several cases in which conventional DW imaging suggested infarcts, but these were determined to be artifacts because they did not appear on thin-section

TABLE 2: Cases in which diagnoses were altered after thin-section DWI

Patient/Sex/Age (y)	Findings			
	Clinical Presentation	Conventional DWI	Thin-Section DWI	Cardiac
1/M/80	Facial paralysis	Normal	Lateral medullary syndrome	None
2/F/78	L facial numbness	Normal	Lacunar	None
3/M/59	R hemiplegia	Normal	Lacunar	None
4/M/70	Transient ischemic attack	Normal	Lacunar	None
5/M/75	Asthenia	Normal	Lacunar	None
6/M/67	Oculomotor nerve palsy	Normal	Lacunar	None
7/M/67	Aphasia	Normal	Large-artery sclerosis	None
8/M/68	Dizziness	Large-artery sclerosis	Cardiogenic embolism	Coronary disease
9/F/77	R hemiplegia	Large-artery sclerosis	Cardiogenic embolism	Atrial fibrillation
10/M/73	Aphasia	Lacunar	Cardiogenic embolism	Atrial fibrillation
11/M/83	L hemiplegia	Lacunar	Branch atheromatous disease	None

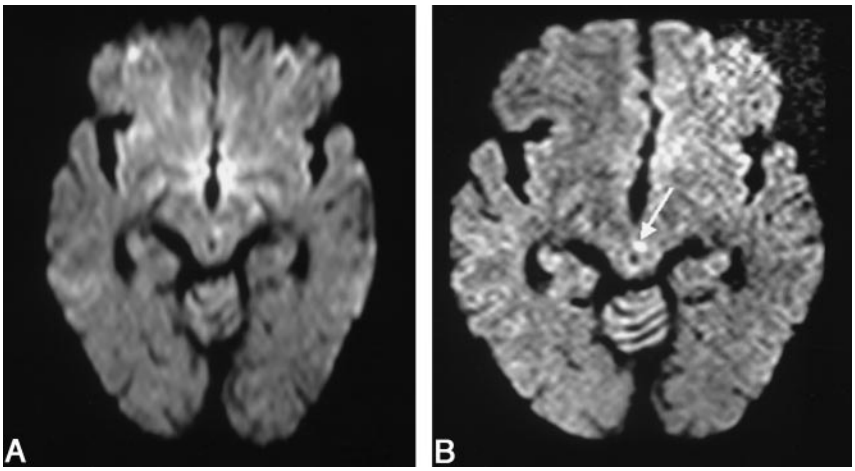

FIG 1. Images in a 67-year-old man with oculomotor nerve palsy.

A, Conventional DW imaging fails to show any significant abnormality.

B, The thin-section DW imaging shows a tiny hyperintense lesion at the left paramedian midbrain (*arrow*). The TOAST diagnosis was changed from normal to small-vessel disease.

DW imaging (Fig 3). These instances are not directly reflected in our data.

In territorial infarction cases, thin-section DW imaging did not prove to be more useful than other studies in determining the TOAST classification. Because territorial infarctions result in larger lesions, conventional DW imaging was sufficient to depict the overall appearance of the lesion. Depiction of any other small infarct in the same vascular territory on thin-section DW imaging would not alter the diagnosis or management. Because of the limited benefit of adding thin-section DW imaging to conventional DW imaging for examining and diagnosing territorial infarcts, the strategy may be to perform thin-section DW imaging only in patients with apparently nonterritorial infarcts. Another strategy is to omit conventional DW imaging and use the thin-section method alone for all stroke cases; this would shorten the total MR imaging examination time. In fact, after completing this study, we changed our stroke protocol to use only thin-section DW imaging.

The major drawback of this technique is the increased imaging time. At our institution, examination time is 1 minute 28 seconds for conventional DW imaging and 4 minutes 24 seconds for thin-section DW imaging. One may argue that the time allowed for imaging in an acute stroke setting is limited and that tripling the imaging time of DW imaging cannot be justified. However, we believe that the added information is important, and we would consider shortening other imaging time than eliminating thin-section DW imaging if the total examination time is an issue.

One study limitation deserves a comment. In our study, the final diagnosis was not reached completely independent of the diagnostic test being evaluated, namely, thin-section DW imaging. As Lee et al (3) pointed out, this is an important limitation, as the results of thin-section DW imaging may influence the choice of complementary tests, such as ultrasonography of heart and neck vessels.

Conclusion

Imaging with thin-section DW imaging increased lesion conspicuity and directly improved the accuracy of stroke subtype diagnosis. Because stoke subtype influences initial management decision, thin-section DW imaging may be advantageous to guide therapy and hospital admission.

Acknowledgments

We are grateful to the technical support by Nobuhiro Kakoi, RT. We also express our special thanks for the invaluable scientific and technical support from Marc Van Cauteren, PhD, Philips Medical Systems.

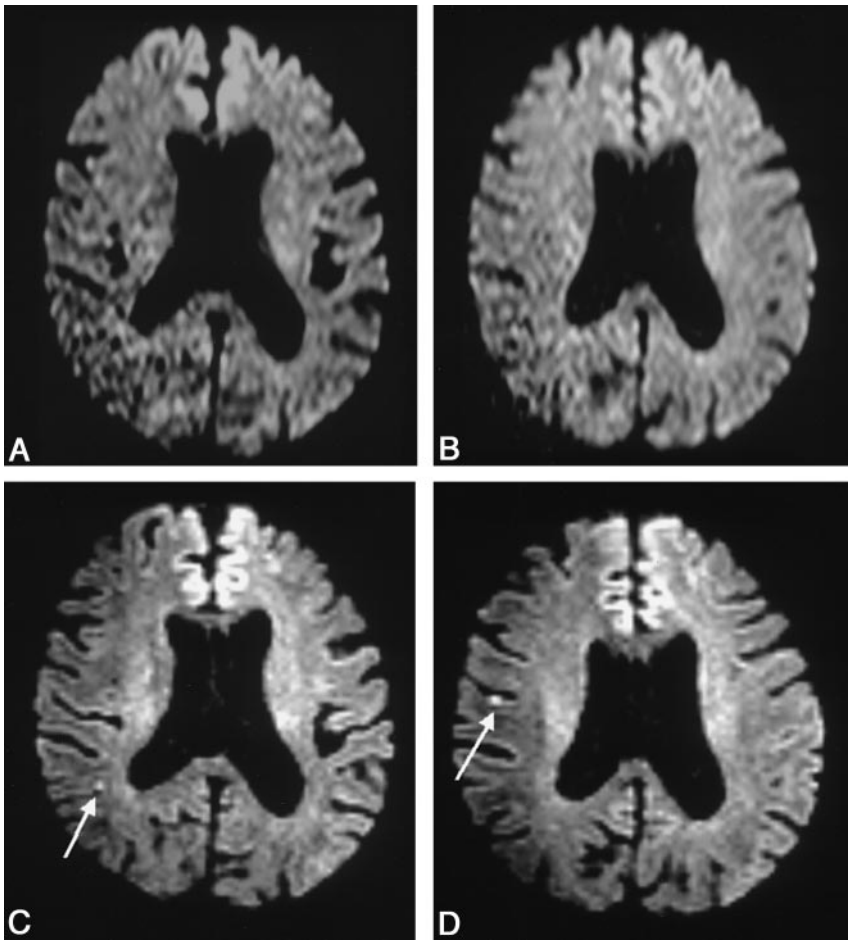

FIG 2. Images obtained in a 67-year-old man with aphasia.

A and *B*, Conventional DW images do not depict any lesions.

C and *D*, Thin-section DW images depict lesions in the cerebral hemisphere in the middle cerebral artery territory (*arrows*). The TOAST diagnosis was changed from normal to large-artery atherosclerosis.

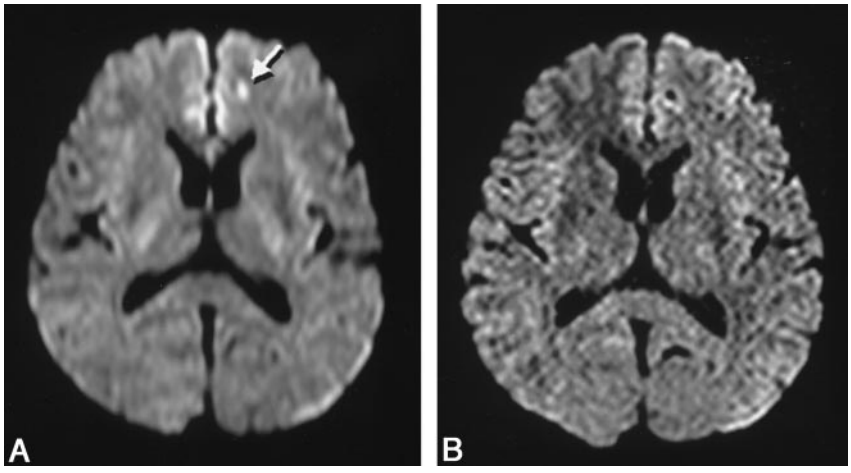

FIG 3. Images obtained in a 45-year-old woman with atrial fibrillation.

A, Conventional DW imaging shows a hyperintense lesion (*arrow*) in the left frontal lobe.

B, Thin-section DW imaging does not show this lesion, and the first finding is determined to be an artifact.

References

1. Moseley ME, Cohen Y, Mintorovitch J, et al. **Early detection of regional cerebral ischemia in cats: comparison of diffusion- and T2-weighted MRI and spectroscopy.** *Magn Reson Med* 1990; 14:330–346
2. Hajnal JV, Doran M, Hall AS, et al. **MR imaging of anisotropically restricted diffusion of water in the nervous system: technical, anatomic, and pathologic considerations.** *J Comput Assist Tomogr* 1991;15:1–18
3. Lee LJ, Kidwell CS, Alger J, Starkman S, Saver JL. **Impact on stroke subtype diagnosis of early diffusion-weighted magnetic resonance imaging and magnetic resonance angiography.** *Stroke* 2000;31:1081–1089
4. Mukherjee P, Bahn MM, McKinstry RC, et al. **Differences between gray matter and white matter water diffusion in stroke: diffusion-tensor MR imaging in 12 patients.** *Radiology* 2000;215:211–220
5. Copen WA, Schwamm LH, Gonzalez RG, et al. **Ischemic stroke: effects of etiology and patient age on the time course of the core apparent diffusion coefficient.** *Radiology* 2001;221:27–34
6. Molyneux PD, Tubridy N, Parker GJ, et al. **The effect of section thickness on MR lesion detection and quantification in multiple sclerosis.** *AJNR Am J Neuroradiol* 1998;19:1715–1720
7. Bradley WG, Glenn BJ. **The effect of variation in slice thickness and interslice gap on MR lesion detection.** *AJNR Am J Neuroradiol* 1987;8:1057–1062
8. Schwartz A, Gass A, Hennerici MG. **Is there a need to reclassify acute stroke patients?** *Cerebrovasc Dis* 1998;8(suppl 1):9–16
9. Pinto AN, Melo TP, Lourenco ME, et al. **Can a clinical classifica-**

tion of stroke predict complications and treatments during hospitalization? *Cerebrovasc Dis* 1998;8:204–209
10. Yamada K, Kubota H, Kizu O, et al. **Effect of intravenous gadolinium-DTPA on diffusion-weighted images: evaluation of normal brain and infarcts.** *Stroke* 2002;33:1799–1802
11. Adams HP Jr, Bendixen BH, Kappelle LJ, et al. **Classification of subtype of acute ischemic stroke: definitions for use in a multicenter clinical trial. TOAST—Trial of Org 10172 in Acute Stroke Treatment.** *Stroke* 1993;24:35–41
12. Madden KP, Karanjia PN, Adams HP Jr, Clarke WR. **Accuracy of initial stroke subtype diagnosis in the TOAST study: Trial of Org 10172 in Acute Stroke Treatment.** *Neurology* 1995;45:1975–1979
13. Baird AE, Lovblad KO, Schlaug G, Edelman RR, Warach S. **Multiple acute stroke syndrome: marker of embolic disease?** *Neurology* 2000;54:674–678
14. Lutsep HL, Albers GW, DeCrespigny A, Kamat GN, Marks MP, Moseley ME. **Clinical utility of diffusion-weighted magnetic resonance imaging in the assessment of ischemic stroke.** *Ann Neurol* 1997;41:574–580
15. Tersei LM, Vogler E, Lipson SA, Bradley WG Jr. **Optimizing scanning techniques and protocols.** In: Stark DD Jr, ed. *Magnetic Resonance Imaging* 3rd ed. St Louis: Mosby; 1999:A1–A13
16. Bradley WG Jr, Atkinson DJ, Edelman RE. **Fast spin-echo and echo-planar imaging.** In: Stark DD Jr, ed. *Magnetic Resonance Imaging.* 3rd ed. St Louis: Mosby; 1999;125–157